THE ASTROPHYSICAL JOURNAL, 478:701–712, 1997 April 1

PULSED $e^{\pm}$ ANNIHILATION γ-RAY LINE FROM A CRAB-LIKE PULSAR

TIANHUA ZHU AND MALVIN RUDERMAN
Physics Department and Columbia Astrophysics Lab, Columbia University, 538 West 120th Street, New York, NY 10027
Received 1995 September 29; accepted 1996 October 17

ABSTRACT

Electron-positron pair production and annihilation within the magnetosphere of a γ-ray pulsar such as the Crab are considered. Outer-magnetosphere accelerator models seem capable of giving both the 10^{40} s^{-1} $e^{\pm}$ pair annihilation rate and the narrow, gravitationally redshifted $e^{\pm}$ annihilation line shape in the Crab pulsar spectrum reported by the FIGARO collaboration. An essential feature is the expected formation of an electron-positron layer well above the pulsar surface, in which gravitational pull toward the star is balanced by cyclotron resonance scattering of polar cap X-rays. Applications to other γ-ray pulsars with smaller spin-down powers than that of the Crab pulsar are also considered.

Subject headings: gamma rays: theory — pulsars: individual (Crab Nebula) — radiation mechanisms: nonthermal — stars: neutron

1. INTRODUCTION

Various proposed pulsar magnetosphere models involve different accelerator and pair production regions. In polar cap models, the accelerator forms relatively close to the neutron star surface within the open field line bundle. Charged particles are accelerated to extremely high energies (about 10^{12} eV) by the electric field of the accelerator. Because they move along the accelerator's curved magnetic field lines, these primaries emit, typically, 10^2 MeV "curvature photons." Electron-positron pairs are produced by these 10^2 MeV photons when they cross the strong neutron star magnetic field in the near magnetosphere:

$$\gamma + \boldsymbol{B} \rightarrow e^+ + e^- + \boldsymbol{B} . \quad (1)$$

The total potential drop of a polar cap accelerator is generally limited by quenching from an $e^{\pm}$ pair production cascade to about 10^{12} V (Ruderman & Sutherland 1975), but it may be somewhat larger in some models.

In outer-magnetosphere accelerator models, charge depletion regions are located faraway from neutron star surface, near the light cylinder (where a corotating magnetosphere would achieve a relativistic velocity). The local magnetic field there is very much weaker than that in a polar cap model, and the $e^{\pm}$ pair production mechanism of equation (1) is not expected to be important. Instead, the accelerator is controlled by pair production from collisions between γ-rays and other γ-rays or X-rays, or, in the case of the Crab pulsar, perhaps optical photons:

$$\gamma + \gamma \rightarrow e^+ + e^- . \quad (2)$$

The total potential drop along the magnetic field of an outer-magnetosphere accelerator is typically more than 2 orders of magnitude larger than that of a polar cap accelerator.

In young pulsars such as the Crab, the Vela, and other γ-ray pulsars, both kinds of accelerators may well exist. The $e^{\pm}$ pair production rate and the annihilation location of the $e^{\pm}$ pairs from a polar cap accelerator, and from an outer-magnetosphere accelerator, seem very different. Then, if confirmed, the very strong, gravitationally redshifted, $e^+ + e^- \rightarrow \gamma + \gamma$ annihilation line in the spectrum of the Crab pulsar reported by the FIGARO (French Italian GAmma Ray Observatory) collaboration (Agrinier et al. 1990 and Massaro et al. 1991) should discriminate between different models for the Crab pulsar magnetosphere.

In § 2, we review briefly the observational history of a pulsed $e^{\pm}$ annihilation line from the Crab pulsar, with special attention to the results of the FIGARO collaboration. In § 3, we consider the gravitationally redshifted $e^{\pm}$ annihilation line expected for outer-magnetosphere accelerator models and show how such models lead to copious $e^{\pm}$ pair production above (but not on) the stellar surface all around the star. In § 4, we show how $e^{\pm}$ annihilation can mainly be in a relatively thin layer above the neutron star's surface. The model's annihilation line strength, redshift, and width are compatible with those reported by the FIGARO collaboration. Some problems in accounting for such an annihilation feature with polar cap models are presented in § 5: annihilation line features of the FIGARO II data are not expected in conventional curvature-induced pair cascade polar cap models (which, however, does not conflict with the OSSE results of the Crab pulsar). In § 6, we consider possible $e^{\pm}$ annihilation radiation from other γ-ray pulsars.

2. OBSERVATIONAL EVIDENCE FOR A PULSED $e^{\pm}$ ANNIHILATION LINE

A possible pulsed γ-ray line at an energy close to, but less than, the rest energy of an electron had been reported often since the discovery of the Crab pulsar. Such a redshifted line could most plausibly come from electron-positron annihilation near the surface of the Crab neutron star. The first reported observation (Leventhal, MacCallum, & Watts 1977) claimed detection of a pulsed Crab pulsar emission line at 0.400 ± 0.001 MeV with an intensity of $(2.2 \pm 0.9) \times 10^{-3}$ photons cm^{-2} s^{-1}. Since then, various observations have either supported the existence of such an annihilation line, but at a different intensity, or put conflicting upper limits to its intensity. Yoshimori et al. (1979) reported an emission line from the Crab pulsar at 0.400 ± 0.002 MeV with an intensity of $(7.4 \pm 5.4) \times 10^{-3}$ photons cm^{-2} s^{-1}, while Ayre et al. (1983) and Owens, Myers, & Thompson (1985) reported a similar emission line with an intensity about $(7.2 \pm 2.1) \times 10^{-3}$ photons cm^{-2} s^{-1}. Harris, Share, & Leising (1994) failed to confirm these observation using the *Solar Maximum Mission* data. Refer-

ences to observations of $e^{\pm}$ annihilation emission line from the Crab pulsar have been collected by Owen (1990).

Such an annihilation line in the spectrum of the Crab pulsar has been reported more recently by the FIGARO collaboration again. The FIGARO experiment was especially designed to study pulsars with a well-established pulse signature period for emission in the energy range 0.2–6.0 MeV. This experiment seems to have the best energy resolution and statistical significance (and has been repeated by this same collaboration with consistent results) among claimed $e^{\pm}$ annihilation line observations.

From both their 1986 July and 1990 July observations, the FIGARO collaboration identified a pulsed emission feature in the spectrum of the Crab pulsar (Massaro et al. 1991; Fig. 1) with the following characteristics:

1. The reported $e^{\pm}$ annihilation line is extremely strong: the observed flux of annihilation photons, $F \simeq (0.86 \pm 0.33) \times 10^{-4}$ photons cm^{-2} s^{-1}, implies an $e^{\pm}$ annihilation rate of 10^{40} s^{-1} in the magnetosphere of the Crab pulsar. This is over 10^6 times greater than the expected Goldreich-Julian charged particle flow out of the pulsar's surface polar caps (Goldreich & Julian 1969).

2. The line is at an energy 0.44 ± 0.01 MeV, redshifted by 70 keV below the rest energy of an electron (positron). This redshift suggests that the annihilation photons escape from the large gravitational potential quite near the surface of the neutron star. If the Crab pulsar is assumed to have a mass 1.4 $M_{\odot}$, the annihilation location that gives this redshift is 16 km above the center of the star, considerably above the generally assumed 10 km pulsar radius. On the other hand, if the annihilation happens at the surface of the neutron star with an assumed radius 10 km, the required mass is only 0.9 $M_{\odot}$. This may be too small for plausible pulsar birth scenarios. (Neutron star masses have been observed to be close to 1.4 $M_{\odot}$ for those neutron stars in binaries that allow a mass determination.)

3. The annihilation line is quite narrow. The FIGARO group's data has been fitted by an emission line plus a power law. The line width in the fit is limited only by the detector resolution, about 59 keV FWHM at the annihilation line energy (Massaro et al. 1991).

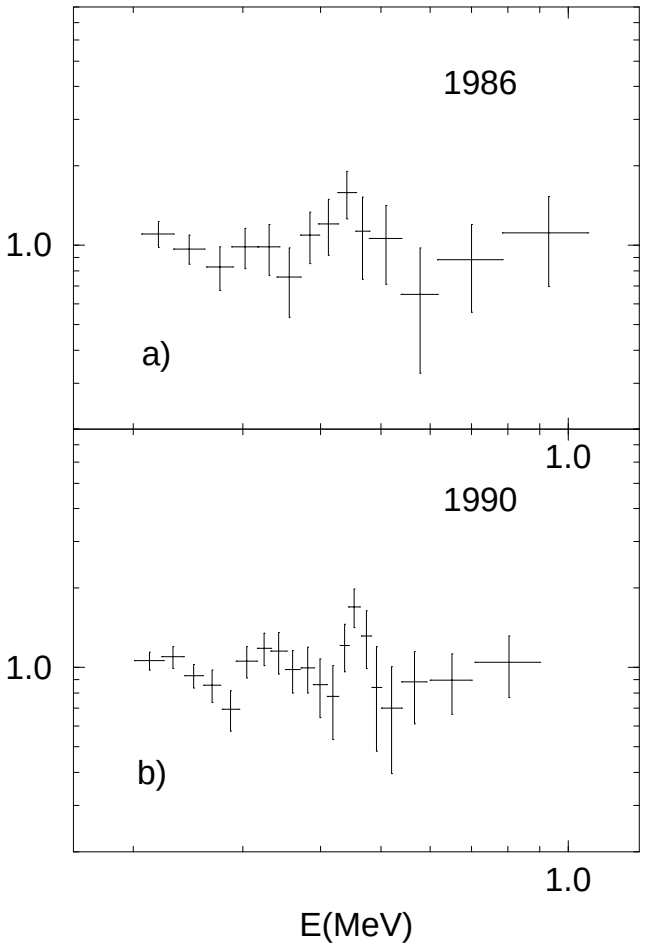

FIG. 1.—Ratio of the net spectra of the Crab photon excess after subtraction of the off-pulse signal to a best power-law fit, for the two FIGARO II flights of (*a*) 1986 July 11 and (*b*) 1990 July 9 (from Massaro et al. 1991).

The discrepancy between reported results of observations at different times suggests that there might be variability in the annihilation emission line from the Crab pulsar. This variability might be related to possible changes in the accelerator that powers the relevant pair production for the annihilation emission.

Observations of the Crab pulsar with OSSE may establish the fluxes or upper limits for the Crab pulsar's redshifted annihilation radiation. Preliminary results from recent OSSE observations (Ulmer 1996) indicate no detectable line present near (± 20 keV) 440 keV (such a line would have been detected if it have been 2–4 times weaker than that observed by FIGARO). This might also suggest variability in the annihilation emission line from the Crab pulsar.

Below, we shall use FIGARO group data to illustrate our model, and we also try to account for the possible variability in the annihilation line.

3. THE $e^{\pm}$ PAIR PRODUCTION FROM OUTER-MAGNETOSPHERE ACCELERATOR AS SOURCE FOR PAIR ANNIHILATION IN NEAR MAGNETOSPHERE

The existence of a powerful accelerator in the Crab pulsar's outer magnetosphere is supported by the pulsar's observed optical luminosity, which exceeds 10^{-5} of its total spin-down power (Cheng, Ho, & Ruderman 1986a and 1986b, hereafter CHRa and CHRb, respectively). The detailed shape and location of an outer-magnetosphere accelerator is uncertain. An outer-magnetosphere gap might develop along the null surface (Cheng, Ruderman, & Sutherland 1976; Cheng & Ruderman 1977), or it might form along the last close field line with a slablike shape (CHRa; CHRb). A mixed type of accelerator that includes both the above gaps may be possible also. Figure 2 shows the possible geometry of the outer-magnetosphere accelerator "gap." The following discussion about $e^{\pm}$ pair production and annihilation does not depend on the detailed geometry of the accelerator. We use the geometry of a slab-shaped outer-magnetosphere accelerator model (CHRa; CHRb) in Figure 2 only to illustrate our discussion, and where relevant, we shall indicate differences among outer-magnetosphere accelerator predictions for different possible structures. We assume that the outer-magnetosphere accelerators develop in order to provide $e^{\pm}$ pairs to support needed magnetosphere current flow.

3.1. *Pair Production inside the Accelerator*

Inside of the accelerator, electrons and positrons are accelerated in opposite directions to extremely high energy

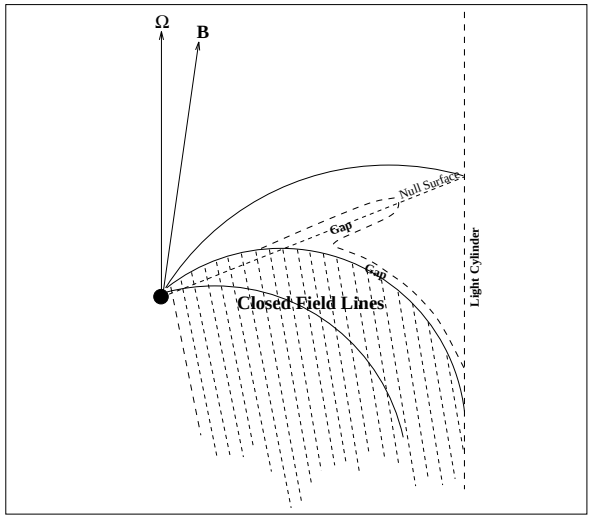

FIG. 2.—The geometry for an outer-magnetosphere accelerator can exist along the null surface or along the last closed magnetic field line, or both. $\boldsymbol{B}$ is the direction of the stellar dipole moment.

when the pulsar outer-magnetosphere electric field $\boldsymbol{E}$ gives a force balanced by curvature radiation reaction. The limiting Lorentz factor γ of the "primary" electrons and positrons is given by

$$e\boldsymbol{E}\cdot\hat{\boldsymbol{B}}c \sim \frac{e^2}{c^3}\gamma^4\left(\frac{c^2}{\rho}\right)^2 , \tag{3}$$

where ρ is the curvature radius of the local magnetic field lines, and $\boldsymbol{E}\cdot\hat{\boldsymbol{B}}$ is the electric field component along $\boldsymbol{B}$. For the Crab pulsar, equation (3) gives γ of the order of 10^7. Curvature photons radiated by the primary electrons and positrons have an energy $\sim\hbar\gamma^3(c/\rho)$. Essentially, the full accelerator potential energy drop $e\Delta V$ would be radiated away in the form of curvation radiation by the primary electrons and positrons. With an accelerator along the last closed field line, each such electron and positron would produce about $N_\gamma \sim (\gamma e^2/\hbar c) \sim 10^5$ curvature photons. To sustain the primary current flow and account for the observed X-ray and γ-ray luminosity from the Crab pulsar, the needed primary particle flux is around 10^{33} s^{-1}. For an accelerator along the null surface, the primary particle flux would be about 10^{34} s^{-1}, the Goldreich-Julian current of the pulsar, and the number of γ-ray photons produced by each primary particle, would be 10 times less. This is the maximum net particle flow through an accelerator regardless of how energy is extracted from it. Clearly, annihilation of these $e^{\pm}$ pairs makes a negligible contribution to the observed annihilation line.

3.2. *Pair Production from GeV γ-Rays and Surface X-Rays*

The $e^{\pm}$ pairs can also be produced through collisions between very high energy γ-rays (greater than 1 GeV) emitted from the outer-magnetosphere accelerator and soft thermal X-rays from the stellar surface of the Crab pulsar. However, because of the strong nonthermal synchrotron X-ray radiation from secondaries, surface emission of soft X-rays from the Crab pulsar should be unimportant in producing $e^{\pm}$ pairs relative to the other mechanisms discussed below. It may, however, play a crucial role in other γ-ray pulsars such as Vela and Geminga.

3.3. *Pair Production from Crossed Outer-Magnetosphere Fan Beams*

Crossed fan photon beams would be formed from the almost symmetrical secondary $e^{\pm}$ flow for the possible geometry shown in Figure 3. Although, in most of the keV-GeV regime, such crossed beams would be optically thin to each other, photon-photon collisions in the crossed beams do produce abundant $e^{\pm}$ pairs when those beams correspond to the observed Crab emission beams. For the Crab pulsar, a tertiary $e^{\pm}$ population from crossed secondary photon beams may also contribute to the high-energy pulsed emission. Half of the pair flux (six in Fig. 3) would flow out of the magetosphere's light cylinder, and the other half (seven in Fig. 3) would flow in along open field lines toward the star and would be expected to annihilate on the polar cap open field line bundle close to the star. Although a large $e^{\pm}$ pair flux can be produced from crossed fan beams, the following two arguments strongly argue against this process being responsible for the reported $e^{\pm}$ annihilation line.

1. A maximum $e^{\pm}$ pair production rate in the Crab pulsar's outer magnetosphere can be estimated from the pulsar's observed optical luminosity of about 10^{33} ergs s^{-1}. Optical photons will be part of the synchrotron radiation from these pairs since pairs are produced in the outer magnetosphere mainly by photon-photon collision, which gives the pairs an important initial momentum component perpendicular to the local $\boldsymbol{B}$. The characteristic synchrotron emission frequency is

$$\omega_c \simeq \gamma^2\frac{eB}{mc}\sin\theta , \tag{4}$$

where $B \sim 10^6$ G is the local magnetic field, γ is the Lorentz factor of electrons or positrons, and θ is the pitch angle of these leptons with respect to the direction of the local magnetic field. This frequency is in the optical regime as soon as γ falls below 10 because of the Crab's strong outer-magnetosphere synchrotron radiation. Then the total flux

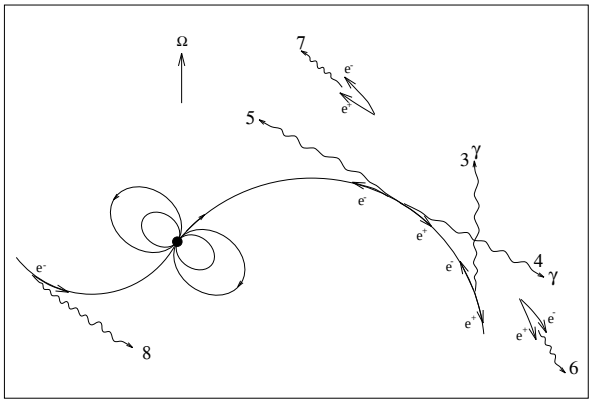

FIG. 3.—One possible geometry for photon emission from outer-magnetosphere accelerators with the geometry of Fig. 2 that accelerates e^- and e^+ oppositely along local $\boldsymbol{B}$. The resulting radiation from curvature radiation, synchrotron radiation, or inverse Compton scattering is a fan covering almost all latitudes. Similar beams go outward (beams 4 and 6) and inward (beams 3 and 7). Because of dipolar symmetry, the observer who sees outward-moving photons in beam 4 in one subpulse may also see inward-moving photons (beam 8) from the other side of the star arriving later in a second subpulse as the star rotates; γ-ray beam crossing, such as shown for beams 3 and 4, sustains some $e^{\pm}$ production around the accelerator.

of such electrons or positrons, needed to account for the observed optical luminosity, would be

$$\dot{N}_{\pm} \simeq \frac{L_{\rm optical}}{\gamma mc^2} \sim 10^{38}\ {\rm s}^{-1}\ , \tag{5}$$

2 orders smaller than the $e^{\pm}$ flux needed for the reported annihilation line.

2. Even if we assume that a $10^{40} e^{\pm}\ {\rm s}^{-1}$ pair production rate could be realized in the outer-magnetosphere region of the Crab pulsar and could move in toward the star, the annihilation of the $e^{\pm}$ still cannot explain satisfactorily the redshift and, especially, the narrow width of the reported annihilation line. The $e^{\pm}$ would approach the stellar surface along the relatively small (area $\sim 10^{10}\ {\rm cm}^{-2}$) bundle of open field lines. If they did not annihilate first, they would be slowed by a shock in the plasma close to the Crab stellar surface. If most electrons and positrons were to annihilate just before passage through the shock, the speed (v) of inflowing $e^{\pm}$ would be at least

$$v \sim \sqrt{\frac{GM_{\rm crab}}{r}} \sim 10^{10}\ {\rm cm\ s}^{-1}\ . \tag{6}$$

Such a large inflow speed would give annihilation line energy shifts varying greatly through the observed pulse (and thus an unacceptably huge line broadening). If the annihilation were to take place after passage through a shock standing above the surface, the postshocked $e^{\pm}$ plasma would be much too hot to give a narrow emission line. Even potentially more serious is that an $e^{\pm}$ inflow of $10^{40}\ {\rm s}^{-1}$ with the speed of equation (6), or less, could form an optically thick column ($n_{\pm} \simeq 10^{20}\ {\rm cm}^{-3}$, $n_{\pm} R_{\rho} \simeq 10^{25}\ {\rm cm}^{-2}$, and the scattering cross section for 0.5 MeV photons $\sigma \simeq 3 \times 10^{-25}\ {\rm cm}^2$) near the stellar surface. Redshifted annihilation γ-rays would then generally scatter and lose much of their energy before escape, and the pulsed narrow line annihilation emission would be strongly diminished.

3.4. *Inner-Magnetosphere Electron-Positron Pair Production and Annihilation as Consequence of Outer-Magnetosphere Accelerator*

The electron flow through an outer-magnetosphere accelerator ($\dot{N}_a$) can be conveniently written as

$$\begin{aligned} \dot{N}_a &\sim f B_p R^3 \Omega^2 e^{-1} c^{-1}\ , \\ &\sim f \times 10^{34}\ {\rm s}^{-1}\ , \end{aligned} \tag{7}$$

with f the fraction of Goldreich-Julian current passing through the accelerator. For a Crab accelerator along the last closed field line, $f \sim 0.1$ (CHRa; CHRb). For an accelerator along the null surface, $f \sim 1$. Within the accelerator, this charged particle flow is accelerated by an electric field whose component along $\boldsymbol{B}$ is $\sim 10^6\ {\rm V\ cm}^{-1}$. The radiation reaction–limited energies of accelerator e^- (or e^+) are large enough to give curvature radiation with γ-ray energies up to several GeV. Coming out of the starward end of the accelerator is a flow $\dot{N}_a \sim f \times 10^{34}\ {\rm s}^{-1}$ of e^- (or e^+) that initially curvature radiates GeV γ-rays. Because $\boldsymbol{E} \cdot \hat{\boldsymbol{B}} \sim 0$ along the open field line path between the inward end of the accelerator and the polar cap, the e^- (or e^+) lose most of their initial energy through curvature radiation. Their instantaneous energy-loss rate ($\dot{E}$) is

$$\dot{E} = \dot{\gamma} mc^2 = -\frac{2c}{3}\left(\frac{e}{\rho}\right)^2 \gamma^4\ , \tag{8}$$

where ρ is again the local curvature radius of the "open" field lines that link the outer-magnetosphere accelerator to the surface polar cap. For a dipole field, $\rho \sim (rc/\Omega)^{1/2}$. When the primaries approach the polar cap, their Lorentz γ is given by

$$\frac{1}{\gamma^3} - \frac{1}{\gamma_a^3} \sim \frac{2\Omega e^2}{mc^3} \ln \frac{r_a}{r}\ , \tag{9}$$

where γ_a is the value of γ when leaving the accelerator at a distance $r_a \sim c\Omega^{-1}$ away from the star, r is the distance of the inflowing e^- (e^+) from the neutron star center, and Ω is the pulsar angular spin rate. As long as $r \ll r_a$, γ is not sensitive to the distance r and is approximately constant along the electron trajectory. For the Crab pulsar near the stellar surface,

$$\gamma \sim \left(\frac{2\Omega e^2}{mc^3} \ln \frac{r_a}{r}\right)^{-1/3} \sim 5 \times 10^6\ . \tag{10}$$

The energy of each curvature-radiated γ-ray as the star is approached is

$$E_{\gamma} \sim \frac{\gamma^3 c^{1/2} \Omega^{1/2} \hbar}{r^{1/2}} \sim 60 \left(\frac{r}{10^7}\right)^{1/2}\ {\rm MeV}\ . \tag{11}$$

The number of such γ-rays radiated over the distance $(rc/\Omega)^{1/2}$ is

$$\frac{\dot{N}_{\gamma}}{\dot{N}_a} \sim \frac{\gamma e^2}{\hbar c} \sim 10^5 \tag{12}$$

for each inflowing e^- (e^+). These γ-rays are radiated in a direction almost exactly parallel to the $\boldsymbol{B}$ along which their source e^- (e^+) moves. Because of the curvature of the magnetic field line, the angle θ between a γ-ray's momentum and the local magnetic field through which it passes increases as the γ-ray approaches the star. The γ-ray will be converted to an $e^{\pm}$ pair as soon as

$$\frac{E_{\gamma} \sin\theta}{2mc^2} \geq 1\ , \tag{13}$$

if

$$B \geq 2 \times 10^{12}\ {\rm G}\ . \tag{14}$$

If equation (14) is not satisfied, then equation (13) must be replaced by

$$\frac{E_{\gamma} \sin\theta}{2mc^2} \frac{B}{2 \times 10^{12}} \geq 1\ . \tag{15}$$

The energy of each of these materialized "secondary" electrons and positrons is about half of the parent γ-ray energy. These secondary electrons and positrons would lose almost all their momentum perpendicular to $\boldsymbol{B}$ immediately by synchrotron radiation in the strong local magnetic field. From equations (13), (14), or (15), the typical energy of the synchrotron γ-rays from the secondaries is

$$\begin{aligned} \hbar\omega_s &\sim \left(\frac{E_{\gamma}}{2mc^2}\right)\left(\frac{E_{\gamma} \sin\theta}{2mc^2}\right)\left(\frac{\hbar eB}{mc}\right)\ , \\ &\sim \left(\frac{E_{\gamma}}{2mc^2}\right)(20\ {\rm keV})\ . \end{aligned} \tag{16}$$

These synchrotron γ-rays from the secondaries would themselves be converted into a third generation of $e^{\pm}$ pairs if the following two criteria are satisfied:

1. The energy of the synchrotron photons exceeds the threshold energy, $2m_e c^2 \sim 1$ MeV, for pair production. From equation (16), this needs

$$E_\gamma \geq 50 \text{ MeV} . \tag{17}$$

2. The synchrotron γ-rays pass across a strong magnetic field, of order 10^{12} G. This condition is fulfilled if the synchrotron photon trajectory passes within about 2 stellar radii of the neutron star. For a pure dipole magnetic field, this condition is met if the radial distance from the star at which the primary curvature γ-ray was emitted satisfies

$$\frac{1}{2}\sqrt{\frac{r^3\Omega}{c}} \leq 2R , \tag{18}$$

or

$$r \leq \left(16R^2 \frac{c}{\Omega}\right)^{1/3} \sim 1.4 \times 10^7 \text{ cm} . \tag{19}$$

After inserting equation (19) into equation (11), we find that $E_\gamma \geq 50$ MeV, which is just the inequality in equation (17). Thus, when $r \leq 1.4 \times 10^7$ cm, both conditions 1 and 2 are satisfied, and almost all of the synchrotron γ-rays from the secondary $e^{\pm}$ pair generation are themselves converted into $e^{\pm}$ pairs. Figure 4 represents the above processes for γ-ray emission and pair production. From equations (7), (11), (12), and (16), the total annihilation γ-ray emission rate around the Crab pulsar is

$$\dot{N}_\gamma = 2\dot{N}_\pm(\text{total}) = 2\dot{N}_a \frac{\gamma e^2}{\hbar c}\frac{E_\gamma}{\hbar\omega_s} \simeq f \times 5 \times 10^{40} \text{ s}^{-1} . \tag{20}$$

This is the annihilation γ-ray emission rate from each hemisphere; the total emission rate from both is then $f \times 10^{41}$ s^{-1}. In the above estimate, we have an almost complete conversion of synchrotron γ-ray photons into $e^{\pm}$ pair rest mass. However, this conversion is rather sensitive to the strength and configuration of the star's magnetic field. The conversion efficiency (f') in various models has values from 0.1 to 1. Then the total pair production rate from both hemispheres, $f \times f' \times 10^{41}$ s^{-1}, is between 10^{39} and 10^{41} s^{-1}, consistent with FIGARO observations. These tertiary electrons and positrons are produced all around the star within several radii of it, and we no longer have the problems associated with an $\dot{N}_\pm$ confined to the very small open field line bundle above the polar caps (the result from crossed fan beams). It is this widely spread $e^{\pm}$ plasma that we propose for the source of the reported $e^{\pm}$ annihilation line. The corresponding annihilation region and the width of the resulting annihilation line are discussed in the next section.

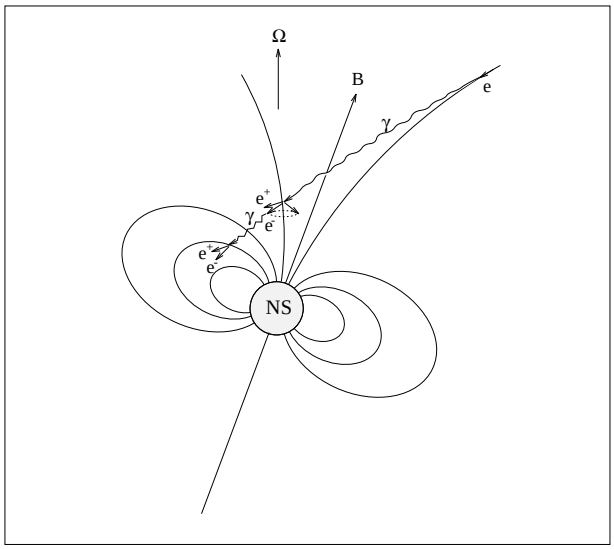

FIG. 4.—γ-ray photons emitted by curvature radiation from inflowing primary particles can be converted into secondary $e^{\pm}$ pairs by passage through the curved magnetic field. MeV photon synchrotron radiation by these secondary electrons and positrons will in turn be transformed into yet another generation of (tertiary) $e^{\pm}$ pairs rather close to the star where the local magnetic fields reach 10^{12} G. Most of these $e^{\pm}$ pairs are created on closed field lines above the star.

Our estimate of the intensity for the gravitationally redshifted annihilation line depends on the activity of the assumed outer-magnetosphere accelerator. As suggested by COS-B observations (Clear et al. 1987; Wills et al. 1982), this activity may well change over time. This might explain the possible variability of the annihilation line for the Crab pulsar.

4. GRAVITATIONAL ENERGY SHIFT AND WIDTH OF ANNIHILATION LINE

In the last section, we showed how the primary particles flowing in toward the star from a presumed outer-magnetosphere accelerator of the Crab pulsar can lead to an $e^{\pm}$ pair production rate of $10^{40\pm1}$ s^{-1} in the near magnetosphere. Most of the $e^{\pm}$ pairs are produced on the closed field lines around the Crab within several radii of the star. Their characteristic lifetime depends upon the $e^{\pm}$ number density ($n_\pm$) there, which varies with location. If these pairs did not move before annihilation, the resulting annihilation line would be too broad, in disagreement with the observation of the FIGARO collaboration. If electrons and positrons did not move before annihilation, the characteristic density of electrons and positrons would be about 10^{17} cm^{-3}, resulting in an e^+ (e^-) lifetime before annihilation of about 10^{-3} s. However, in that time e^+ (e^-) could move up to $30R$ from where they were produced, a distance much larger than the radius of the strongest pair production and annihilation regions (see below). This transport distance is much diminished both by the constraint that $e^{\pm}$ streaming is mainly confined to $\boldsymbol{B}$-field lines and by the increased annihilation rate, where local $n_\pm$ is greater than 10^{17}cm^{-3}. Below, we simply assume that the time before a given e^+ (e^-) annihilates is sufficient for it to adjust its position so that the quasi-steady distribution described in this section can be achieved.

Four kinds of force may act on these electrons and positrons. Because of the strong magnetic field near the surface of the star, charged particles are confined to move only along local magnetic field lines. Thus, only the other force components along the magnetic field line affect particle motion significantly:

1. The attractive gravitational force of the neutron star,

$$\boldsymbol{F}_g = -\frac{GMm}{r^3}\boldsymbol{r} , \tag{21}$$

where M is the mass of the Crab pulsar, m is the mass of an electron (positron), and $\boldsymbol{r}$ is the vector distance of a lepton from the center of the star.

2. The centrifugal force

$$\boldsymbol{F}_c = m\Omega^2 \boldsymbol{r} \tag{22}$$

in the magnetosphere corotating with the star, where Ω is the angular rotation velocity of the star.

3. The radiation force from the e^+ (e^-) scattering of strong surface X-ray emission.

4. The force from any electric field ($\boldsymbol{E}$) along a magnetic field line

$$\boldsymbol{F}_E = q\boldsymbol{E} \cdot \hat{\boldsymbol{B}} \,. \tag{23}$$

The electric force on electrons and positrons is opposite, while all the other forces are the same on both. Where there is an electric field along a magnetic field line, electrons and positrons move in opposite directions. Wherever there are both electrons and positrons in equilibrium, except for annihilation and production, they adjust their distribution so that the parallel component of electric field vanishes: the electric field becomes perpendicular to the magnetic field. Therefore, since there is sufficient $e^{\pm}$ pair production in the near magnetic field region for such field adjustment, we simply neglect the electric force along $\boldsymbol{B}$. The centrifugal force increases with distance from the star, while the gravitational force decreases with distance. The radius where the centrifugal force becomes comparable to the gravitational force is about

$$r = \left(\frac{GM}{\Omega^2}\right)^{1/3} \,. \tag{24}$$

For a 1.4 $M_\odot$ Crab pulsar, this gives $r \sim 1.7 \times 10^7$cm. Because the region of major interest considered below is well within this radius, we shall neglect the centrifugal force there.

Modeling the force from radiation pressure is more complicated. If there were no strong magnetic field, the scattering cross section of electrons and positrons would be the Thomson cross section. However, in the strong magnetic field of the near magnetosphere, X-ray photons interact resonantly with electrons and positrons wherever the photon frequency equals the electron cyclotron frequency. This resonant scattering enhances greatly the radiation pressure on the $e^{\pm}$ plasma in the near magnetosphere. Sturner & Dermer (1994a, 1994b) have studied in detail the consequences of such resonant scattering in supporting an atmosphere around an accreting X-ray pulsar. Key points in their paper are similar to those that are important for the support of an atmosphere resulting from inflowing and locally produced $e^{\pm}$ pair, but they lead to quantitatively very different results in the two cases.

Because of the continuous creation and annihilation of positron-electron pairs in the near magnetosphere of the Crab pulsar, the problem there is more complicated. In addition, the weak gravitational force on electrons and positrons, instead of that on heavier atoms, is balanced by the radiation force.

The polar cap areas of the Crab pulsar are impacted by the primary inflow ($\dot{N}_a$) of e^- (e^+). Each inflowing particle brings in an energy

$$E(R) \simeq mc^2 \left(\frac{2\Omega e^2}{mc^3} \ln \frac{r_a}{R}\right)^{-1/3} \sim 4 \text{ ergs} \,. \tag{25}$$

Then the total emission from the Crab pulsar's polar caps should be $4f \times 10^{34}$ ergs s^{-1} of soft X-rays. The typical energy of those soft X-rays would of the order of 1 keV. Assuming blackbody radiation with temperature kT, the spectrum intensity of X-rays emitted from polar caps is

$$I(\omega) = \frac{15}{\pi^4} \frac{\hbar^4 \omega^3}{(kT)^4} \frac{4f \times 10^{34}}{\exp(\hbar\omega/kT) - 1} \text{ ergs} \,. \tag{26}$$

X-rays are also emitted from the other parts of the stellar surface that have a much lower temperature. These soft X-rays can also interact resonantly with magnetosphere electrons and positrons, but at larger distances from the star than polar cap X-rays. Most of the $e^{\pm}$ pairs are produced on closed field lines within 2–3 radii of the center of the star, and these charge particles are confined to flow along these magnetic field lines. The fraction of pairs produced at these radii, on the closed field lines of a dipole that can flow out to n times those radii, is roughly $(2n)^{-1}$. For a stellar surface temperature (outside the polar caps) of, say, $T \sim 10^6$ K, the resonant X-ray interactions would occur at radii up to several times farther out than the $e^{\pm}$ production radii, so that the pair density is greatly reduced there. Only the first generation of the pairs could easily reach the region where this very soft component interacts resonantly with electrons and positrons, and that pair flux is by itself too small to contribute significantly to the observed $e^{\pm}$ annihilation line.

Therefore, we neglect the consequences of the very soft total area radiation here. Because of gravitational bending, harder X-ray radiation from the two polar caps could illuminate most of the closed field lines. For simplicity, we assume below that the radiation from the two polar caps gives an isotropic distribution with respect to the star. Near the star, this is not a good quantitative assumption. However, our purpose here is not a definitive numerical result (already precluded because we do not know the surface magnetic field distribution), but to show how the electron-positron plasma could accumulate at that distance from the star where annihilation can give a narrow gravitationally redshifted spectral line similar to that in the FIGARO data.

For simplicity, we assume a central dipole magnetic field outside of the star:

$$\begin{aligned} B(r, \theta) &= \frac{B_p}{2} \left(\frac{R}{r}\right)^3 (2 \cos \theta \boldsymbol{e}_r + \sin \theta \boldsymbol{e}_\theta) \\ &\simeq 1.5 \times 10^{12} \left(\frac{R}{r}\right)^3 (2 \cos \theta \boldsymbol{e}_r + \sin \theta \boldsymbol{e}_\theta) \,, \end{aligned} \tag{27}$$

with $B_p \sim 3 \times 10^{12}$ G so that the stellar dipole moment is consistent with the observed Crab pulsar spin-down power. The resonant part of the cross section for the X-ray scattering on an electron (positron) in a magnetic field $\boldsymbol{B}$ can be well approximated as (Blandford & Scharlemann 1976)

$$\sigma \simeq \frac{2\pi^2 e^2}{mc} \delta(\omega_B - \omega) |\hat{\boldsymbol{e}} \times \hat{\boldsymbol{B}}|^2 \,, \tag{28}$$

with $\omega_B = eB/mc$, and $\hat{\boldsymbol{e}}$ the photon polarization. In the optically thin case, the radiation force (averaged over polarization) from $I(\omega)$ of equation (26) on each electron or positron in the magnetic dipole field ($\boldsymbol{B}$) is

$$\boldsymbol{F}_r = \frac{\pi e^2}{4mc^2} \frac{1 + 7 \cos^2 \theta}{1 + 3 \cos^2 \theta} \frac{I(\omega_B)}{r^3} \boldsymbol{r} \,. \tag{29}$$

Figure 5*a* shows this resonant radiation force (averaged over all direction) on an electron (positron) in the optically thin limit, and the gravitational force, at various distances

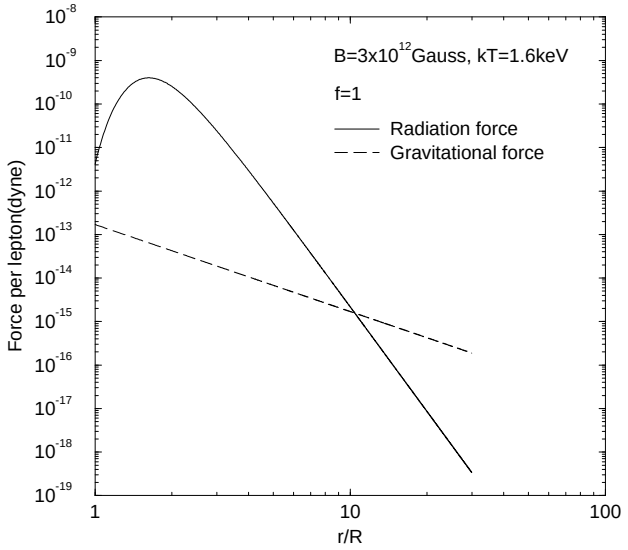

FIG. 5a

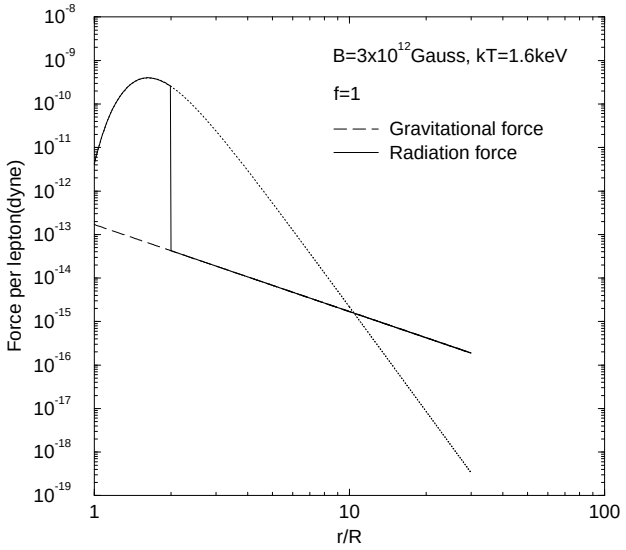

FIG. 5b

FIG. 5.—The radiation force of eq. (29) (averaged over all directions) and the gravitational attraction on e^-/e^+ as a function of distance r from the neutron star center. (*a*) The optically thin limit. An equilibrium radius at which the radiation force equals the gravitational force exists $10R$ away from the star. Below this radius, the radiation push is stronger than the gravitational pull, and the $e^{\pm}$ pairs there will be pushed toward the equilibrium radius. Above the equilibrium radius, they would also be pulled toward the equilibrium radius. (*b*) An optically thick case. The local electron-positron density reaches the maximum supportable pair density at those radii where the net radiation force per lepton equals the gravitational force. In the case illustrated, the force on an e^+/e^- is given by the solid line. The layer is optically thick from $r \simeq 2R$ (a radius that will shrink as more pairs are added) to $r \simeq 10R$ (the optically thin "equilibrium radius" for the indicated X-ray intensity).

from the center of the star. The radiation force balances the gravitational force at $r \simeq 10R$. For $r < 10R$, the radiation force is larger than the gravitational one, while for $r > 10R$, the gravitational force is larger than the radiation force. Thus, in the optically thin case, electrons and positrons produced below $10R$ will be pushed out along their magnetic field line either to the maximum distance away from the star of that field line or out to $10R$ away, whichever is smaller. Those pairs produced above $r \simeq 10R$ will be pulled down toward $10R$. If the number density of electrons and positrons is large enough, the $e^{\pm}$ plasma is optically thick to resonantly scattering photons. When this happens, equation (29) no longer holds. To make an optically thick plasma for resonantly scattering photons at (r, θ), the minimum number density of $e^{\pm}$ is

$$n_t(r, \theta) = 1.6 \times 10^{14} \left(\frac{r}{R}\right)^4 \frac{(1 + 3\cos^2\theta)^{3/2}}{1 + 7\cos^2\theta} \text{ cm}^{-3} . \quad (30)$$

In the near magnetosphere of the Crab pulsar with a $10^{40} e^{\pm}$ s^{-1} pair production rate, the typical electron-positron density is about 10^{17} cm^{-3}, well above that of equation (30). As the $e^{\pm}$ density grows, the radiation force per lepton becomes smaller. At each radius, the maximum pair density that can be supported by the radiation force is reached when the radiation force is equal the gravitational pull. This is illustrated in Figure 5*b*, in which the pair density above $r \simeq 2R$ is the maximum supportable one, while at $r < 2R$, there are no absorbing pairs, so that the radiation force is still that of equation (29). The slow addition of mobile pairs to a stable resonance-supported $e^{\pm}$ layer would cause that layer to grow by moving the added pairs to a slightly smaller radius. Only the inner boundary of the layer decreases, but the rest of the layer is unaffected. The maximum supportable density is achieved when almost all momenta of resonance-scattered X-ray photons are used to support the $e^{\pm}$ plasma:

$$n_{\max}(r, \theta) = 2.6 \times 10^{21} f \times \left[\frac{B_{12}}{kT(\text{keV})}\right]^4 \left(\frac{R}{r}\right)^{13} \times \frac{1}{\exp\left[11.6 B_{12}(R/r)^3/kT(\text{keV})\right] - 1} \text{ cm}^{-3} , \quad (31)$$

where $B_{12} = (B_p/2)(1 + 3\cos^2\theta)^{1/2}$. Figure 6 shows the angle-averaged maximum supportable electron-positron number density $n_{\max}$ as a function of radius from the star. If

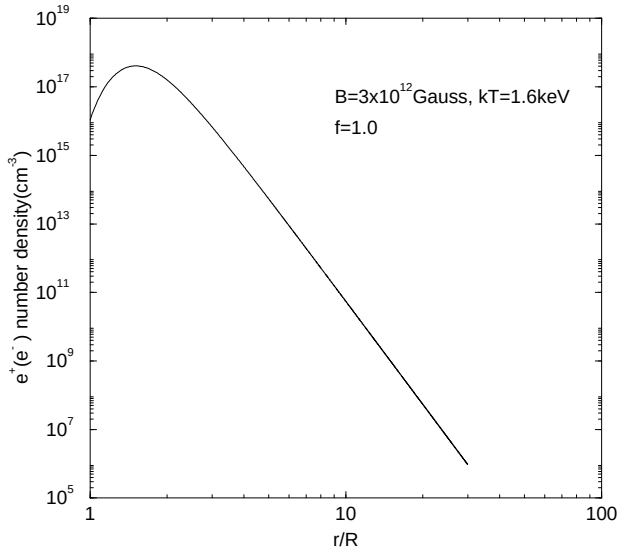

FIG. 6.—The maximum, angle averaged, electron-positron number density that can be supported by the radiation force as a function of radius (r).

the local density of $e^{\pm}$ pairs is larger than the maximum supportable value $n_{\max}$, pairs will be pulled toward the star; otherwise, they will be pushed away from the star. We assume that when a steady state is reached, the local number density will be near the maximum supportable value. The corresponding positron-electron annihilation rate per unit volume ($f_{\rm ph}$) is then given by

$$f_{\rm ph}(r, \theta) = 2\pi\left(\frac{e^2}{mc^2}\right)^2 cn^2(r, \theta) . \quad (32)$$

Because of the gravitational redshift, annihilation photons emitted from electron-positron annihilation at a distance r are observed to have an energy

$$E = mc^2\left(1 - \frac{2GM}{rc^2}\right)^{1/2} . \quad (33)$$

Then the intensity spectrum of annihilation photons is

$$f(E) = \frac{4\pi^2 e^4 Er^4}{GMm^4c^5}\int_0^{\pi} n^2(r, \theta)\sin\theta\, d\theta . \quad (34)$$

This is shown in Figure 7 for $n = n_{\max}$ at all r for various polar cap kT. The total annihilation γ-ray emission rates for $kT = 1.0$, 1.6, and 2.0 keV are $5.1 \times 10^{40} f^2$, $4.4 \times 10^{40} f^2$, and $4.1 \times 10^{40} f^2$ s^{-1}, respectively. For $kT = 1.6$ keV, the peak energy of the spectrum is at 0.44 MeV, in agreement with the result of the FIGARO group. The calculated annihilation line half-width, from the different gravitational redshifts at the various radii at which annihilation occurs, does not exceed the detector resolution (about 59 keV FWHM) of the FIGARO group. Thus, all the essential features of the $e^{\pm}$ annihilation emission line from the Crab pulsar reported by the FIGARO group can be fitted by plausible kT and f.

Another contribution to the emission line width comes from motion of e^+ and e^- along $\boldsymbol{B}$. Electrons and positrons would be expected to be produced with a velocity component along $\boldsymbol{B}$ that is a significant fraction of c. However, the large drag force from the resonant Compton X-ray scattering will bring them to very nonrelativistic speeds on a short timescale. Assuming that at each point the electron and positron density equals the maximum supportable value of equation (31), then at each radius the outflowing photon flux with $\omega < \omega_B(r)$ has not yet been scattered and is therefore still equal to its original value. Photons with $\omega > \omega_B(r)$ have already passed their (optically thick) resonant scattering layer, so this part of the outgoing flux has been greatly diminished. The outflowing photon intensity flux at radius r in a very optically thick region is then

$$I_{\rm out}(\omega, r) \simeq \begin{cases} \dfrac{15}{4\pi^5 r^2}\dfrac{\hbar^4\omega^3}{(kT)^4}\dfrac{L_{\rm x}}{\exp(\hbar\omega/kT) - 1} & \text{for } \omega < \omega_B(r) , \\ \dfrac{GMm}{r^2}\dfrac{mc^2}{2\pi^2 e^2} & \text{for } \omega > \omega_B(r) . \end{cases} \quad (35)$$

There is also a backscattered flow of resonantly scattered photons flowing inward. For $\omega < \omega_B(r)$, the backscattered photon flux would be close to, but smaller than, $I_{\rm out}$ (for a large optical depth). When $\omega > \omega_B$, there is not yet any photon backflow. Thus,

$$I_{\rm in}(\omega, r) \simeq \begin{cases} \dfrac{15}{4\pi^5 r^2}\dfrac{\hbar^4\omega^3}{(kT)^4}\dfrac{L_{\rm x}}{\exp(\hbar\omega/kT) - 1} - \dfrac{GMm}{r^2}\dfrac{mc^2}{2\pi^2 e^2} & \text{for } \omega < \omega_B(r) , \\ 0 & \text{for } \omega > \omega_B(r) . \end{cases} \quad (36)$$

Figure 8 shows $I_{\rm out}$ at $r = 1.7R$, $\theta = \pi/2$ for a Crab polar cap X-ray luminosity ($L_{\rm x}$) of 4×10^{34} ergs s^{-1} with $kT = 1.6$ keV. ($I_{\rm in}$ has a similar shape.) Those electrons and positrons that are essentially at rest would resonantly scatter both inward and outward flowing photons of frequency ω_B. The net radiation force on these pairs balances the gravitational one. However, an electron or positron that was produced initially flowing inward with a large velocity

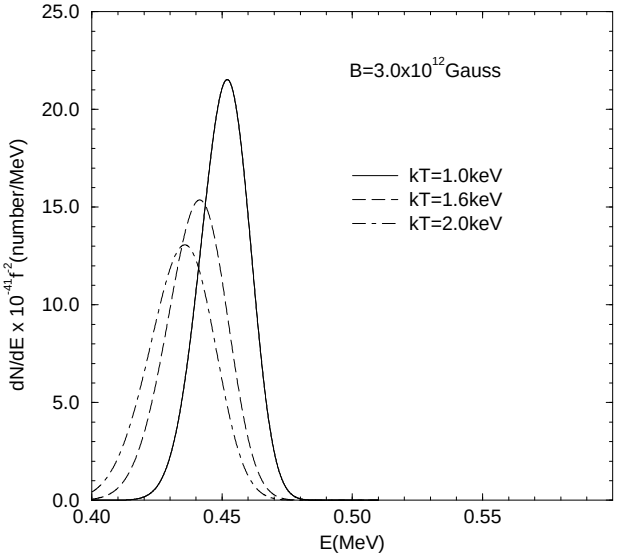

FIG. 7.—Annihilation photon number flux spectra for three different polar cap temperatures, assuming the electron-positron density at each radius equals the maximum supportable one. The total annihilation γ-ray emission rates for $kT = 1.0$, 1.6, and 2.0 keV are $5.1 \times 10^{40} f^2$, $4.4 \times 10^{40} f^2$, and $4.1 \times 10^{40} f^2$ s^{-1}, respectively; $kT = 1.6$ keV gives the best fit to FIGARO observations. The line width is wider for larger polar cap temperatures.

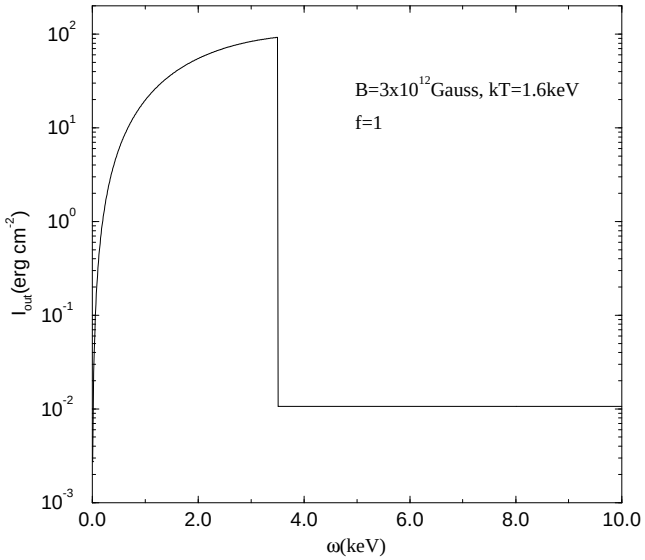

FIG. 8.—The intensity flux spectrum of photons flowing away from the star at $r = 1.7R$. Backscattering flux flowing in toward the star has a similar shape.

along $\boldsymbol{B}$ would scatter resonantly on inward flowing photons of frequency $\omega_B(1 + v/c)$ and outward flowing photons of frequency $\omega_B(1 - v/c)$ only. As long as v is larger than the typical velocity of ambient electrons and positrons, the newly produced particles would be pushed back strongly by the now unbalanced radiation force until their velocity along $\boldsymbol{B}$ is about the same as that of the ambient ones. The characteristic timescale for the $e^{\pm}$ to lose their large initial velocity along $\boldsymbol{B}$ and come to equilibrium with the slow ambient resonantly scattering pairs is then, approximately,

$$t \simeq \frac{mv}{F_r(r)}, \tag{37}$$

with $F_r(r)$ the radiation force of equation (29). This timescale as a function of radius is shown in Figure 9, with $v = c$, together with the lifetime of positrons and electrons before annihilation. Where the ambient $e^{\pm}$ plasma density is high, the new inflowing electrons and positrons lose their kinetic energy before annihilation, even for $v = c$ (which, generally, greatly overestimates the initial particle speed along $\boldsymbol{B}$). If, instead of initially inflowing pairs, we have initially outflowing pairs, $v \rightarrow -v$, the conclusion is the same. For a radiation-supported $e^{\pm}$ plasma equilibrium temperature of 1 keV, similar to that of the polar cap, the thermal contribution to the annihilation line width would be about 40 keV. However, when the incident X-ray radiation intensity from the polar cap is only 10^{-3} of that of keV blackbody radiation from the whole surface of the star, the equilibrium temperature in the plasma would be an order of magnitude less. The contribution to the $e^{\pm}$ annihilation line width from thermal pair motion would, therefore, not be expected to be important for the Crab pulsar, but further study of the "thermal" annihilation line width is needed for a more quantitative estimate.

If the activity of the outer-magnetosphere accelerator changes with time, more $e^{\pm}$ pairs would be produced near the star during intervals of high activity, and less would be produced during periods of low activity. When the production rate of the $e^{\pm}$ pairs around the surface of the star exceeds the maximum supportable $e^{\pm}$ plasma of equation (31), most of the excess pairs would be annihilated on the surface and give a larger redshift. Our model implies a relationship between the intensity and the redshift of the annihilation line: the stronger the intensity, the larger the redshift. This trend seems in agreement with observations.

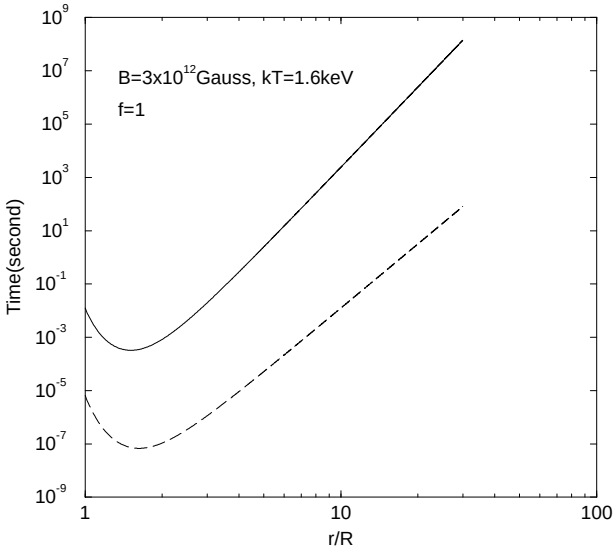

FIG. 9.—Timescale for e^+ (e^-) to lose an initial velocity $v \sim c$ along $\boldsymbol{B}$ at each radius (*dashed line*), and the lifetime of electrons and positrons before annihilation as a function of radius (*solid line*). Local electron-positron densities are assumed to be the maximum supportable ones.

5. SOME DIFFICULTIES IN ACCOUNTING FOR REPORTED $e^{\pm}$ ANNIHILATION LINE BY FIGARO COLLABORATION IN CURVATURE-INDUCED PAIR CASCADE POLAR CAP MODELS

Essential features of the above outer-magnetosphere accelerator model description of the origin and magnitude of the reported narrow, redshifted, pulsed annihilation line from the Crab pulsar include the following:

1. There is an inward flow toward the neutron star of 10^6 $e^{\pm}$ for each e^+/e^- passing through the accelerator. (A smaller multiplicity than 10^6 would not produce the reported 10^{40} s^{-1} γ-rays emission.)
2. The $e^{\pm}$ production and annihilation are mainly on the closed field lines above the stellar surface, and the annihilation region is optically thin for the annihilation γ-rays (but not, of course, to surface emitted X-rays).
3. The annihilation is mainly in a thin blanket about $0.6R$ above the stellar surface. The radii at which most of the annihilation occurs is limited enough to give a sufficiently narrow distribution of gravitational redshifts for the observed annihilation γ-rays.

All of these features appear to be much more difficult to achieve in canonical curvature-induced pair cascade polar cap accelerator models for the origin of the main $e^{\pm}$ pairs. Below, we briefly summarize some of these difficulties:

1. The needed total $e^{\pm}$ pair annihilation rate derived from the FIGARO observational data seems too large to be accommodated in a canonical polar cap model for outflowing $e^{\pm}$ pairs above (or in) the accelerator.The Goldreich-Julian charge density in the polar cap region of a pulsar is $\simeq -\boldsymbol{\Omega} \cdot \boldsymbol{B}_p/2\pi c$. This gives an upper limit to the net particle flow ($\dot{N}_{\rm pc}$) through a polar cap accelerator that does not quench the accelerator,

$$\dot{N}_{\rm pc} \simeq \frac{\Omega^2 B_p R^3}{2ce}, \tag{38}$$

where B_p is the magnetic field strength on the polar cap. For the Crab pulsar, equation (38) gives an upper limit of 10^{34} s^{-1} for particle flow through the pulsar's open field line accelerator. Equation (38) is expected to hold for any surface field distribution with a dipole moment $B_p R^3$ adjusted to fit the observed Crab pulsar spin-down rate. On the other hand, the total potential drop through a polar cap accelerator is generally limited by $e^{\pm}$ pair production to $\Delta V \leq$ a few $\times 10^{12}$ V for the moderately strongly magnetized Crab pulsar. (The ΔV could be somewhat decreased if the field line curvature radius is very much less than that for a pure central dipole.) Then the total power extracted from a Crab pulsar polar cap accelerator $e\dot{N}_{\rm pc}\Delta V \leq 10^{34}$ergs s^{-1}. With 100% efficiency for conversion of polar cap–powered γ-rays into $e^{\pm}$ rest mass, this accelerator might

give the needed 10^{40} s^{-1} $e^{\pm}$ pair production rate. However, the actual conversion efficiency for plausible polar cap models is much smaller. (Most of the curvature γ-rays would be transformed into $e^{\pm}$ pairs by 10^2 MeV curvature γ-rays [Arons 1981; Sturrock 1971; Ruderman & Sutherland 1975]. If each 10^2 MeV γ-ray photon produced one pair, the maximum $e^{\pm}$ pair flux would be less than 10^{34} ergs s^{-1}/10^2 MeV $\sim$ 10^{38} s^{-1}, 2 orders of magnitude smaller than the pair flux needed for the FIGARO-reported annihilation line. Further $e^{\pm}$ production by the synchrotron radiation from these secondaries is much more difficult than in the model considered in § 3 because the local magnetic field is becoming so much smaller for the outward-moving polar cap–induced shower.)

2. To get a strong, narrow enough, but strongly gravitationally redshifted, $e^{\pm}$ annihilation line, we need a copious pair flow that ultimately approaches the stellar surface at nonrelativistic speeds (v). If the flow is confined to the open field line bundle, certainly the case for $e^{\pm}$ production from polar cap accelerators, then the pair annihilation rate ($N_{\pm}$) must satisfy the inequality

$$\dot{N}_{\pm} \leq v n_{\pm} R_p^2 , \tag{39}$$

where $R_p = R(R\Omega/c)^{1/2}$ is the polar cap radius. For the Crab pulsar with $N_{\pm} \sim 2 \times 10^{40}$ s^{-1} (about half of the annihilation γ-rays would not escape), $n_{\pm} R_p > \dot{N}_{\pm}/vR_p \geq 10^{25}$ cm^{-2}, so that the annihilation column may not be optically thin for γ-rays not moving almost perpendicularly to the field line bundle. (For $E_{\gamma} \sim mc^2$, even a single scatter would remove the γ-ray from the observed narrow annihilation line feature.)

3. It is unclear how polar cap models could give the reported annihilation line redshift.

It is plausible to attribute the redshift of the reported $e^{\pm}$ annihilation line to the strong gravitational potential near the surface of the neutron star. However, to do so, the annihilating $e^{\pm}$ pairs have to satisfy two conditions: (1) The electrons and positrons must annihilate well within 2 radii of the star. Otherwise, the gravitational redshift would be too small. (2) The $e^{\pm}$ pairs must move at nonrelativistic speeds when they annihilate. If they move with relativistic speeds, the annihilation energy is increased, and the resulting Doppler shift of annihilation γ-rays would overwhelm the gravitational shift in almost all directions: the model would then not reproduce the observed narrowness of the redshifted annihilation line in the Crab's pulsed spectrum. Outflowing electrons and positrons from canonical polar cap accelerator models satisfy neither of the conditions. The pairs are almost all created moving out, away from the surface of the star, and would not annihilate appreciably before leaving the magnetosphere unless their outflow is reversed. (Most of the electron and positron pairs produced by 10^2 MeV curvature γ-rays move with extremely relativistic velocities: if they annihilate in flight, the gravitational redshift would not be dominant.) If some positrons (or pairs) are turned back and flow into the star through the accelerator, they could not give an inward particle flow back through the accelerator greater than the 10^{34} s^{-1} of equation (38), and this $e^{\pm}$ annihilation rate is insignificant.

4. The positrons or electrons (depending on the angle between the spin axis and the magnetic moment) that are created in or pass through the accelerator itself may flow back onto the polar cap and produce copious positrons through an $e^{\pm}$ shower in the surface crust. However, if these particles have a high energy, the resulting shower would develop well below the polar cap surface. Those few annihilation γ-rays that get back out of the surface would be scattered to lower energy and also greatly broaden the annihilation line width.

A backflow model (Bednarek, Cremonesi, & Treves 1992) that uses a polar cap accelerator for $e^{\pm}$ pair production has been proposed to account for the reported electron-positron annihilation line. In this model, a particle flow of 3×10^{32} s^{-1} of "primary" electrons generated in an outer-magnetosphere accelerator was assumed to move toward the star along magnetic field lines of the open field bundle. Each of these electrons was estimated to produce about 10^3 $e^{\pm}$ pairs on its way toward the star. Most of these particles were assumed to enter into the polar cap accelerator, where each e^- (e^+) will get energy from the accelerator and lose energy by inverse Compton scattering on surface X-rays. With an appropriate surface temperature and polar cap potential drop, each electron (or positron) moving into the polar cap could produce 10^5 photons with energy close to 1 MeV. Once those photons strike the star surface, they would be transformed into $e^{\pm}$ pairs. The positron production rate was estimated to be as high as 3×10^{40} s^{-1}. Those positrons would first lose most of their kinetic energy and then annihilate to give the reported annihilation emission. A serious problem with this model is that the large particle flow ($3 \times 10^{32} \times 10^3 = 3 \times 10^{35}$ s^{-1} passing through the polar cap accelerator is larger than the full Goldreich-Julian current flow of eq. [38]) would be expected to quench the accelerator. This is a general problem for any magnetosphere model that assumes a strong polar cap accelerator and a strong outer-magnetosphere accelerator that span a common bundle of open field lines: $e^{\pm}$ pairs from one of the accelerators would flow to and quench the other accelerator so that both would not coexist.

6. OTHER PULSARS

The γ-ray properties of the Geminga pulsar are consistent with a powerful accelerator in that pulsar's outer magnetosphere. If this is indeed the case, its probably at high efficiency, for converting this pulsar's spin-down power into γ-ray emission would require its outer-magnetosphere accelerator to span a good fraction of accessible open field lines so that the gap types of Figure 2 may merge into a single large region. The primary particle flow through the accelerator may then be a good fraction of the pulsar's maximum Goldreich-Julian net particle flow,

$$\dot{N}_a \sim \frac{B_p R^3 \Omega^2}{ec} \sim 8 \times 10^{31} \text{ s}^{-1} . \tag{40}$$

From equation (20), the $e^{\pm}$ pair production rate in the near-magnetosphere region of the Geminga pulsar, by its curvature γ-rays from inflowing primary e^- (e^+), might then be as high as 8×10^{38} s^{-1}, about 1 order smaller than that of the Crab pulsar. However, at an estimated distance of about 200 pc (Halpern & Ruderman 1993; Bignami, Caraveo, & Mereghetti 1993), the Geminga pulsar is much closer, so that such an $e^{\pm}$ annihilation photon flux from the Geminga pulsar might give an observed line even stronger than that

from the Crab pulsar. Such a Geminga model assumes that the primary particles flowing starward in from the outer-magnetosphere accelerator still have the high energy of equation (25), $E(R) \simeq 6.5$ergs, when they hit the Geminga stellar surface. The power brought down to the polar cap by this inflow would then be

$$L_p \sim N_a E(R) \sim 2 \times 10^{32} \text{ ergs s}^{-1} , \quad (41)$$

several times larger than Geminga's total observed soft X-ray luminosity of about 4×10^{31} ergs s^{-1} for a Geminga distance of 200 pc. This discrepancy may be the result of any of the following origins:

1. There may be a significant perpendicular (to $\boldsymbol{B}$) component of momentum for the leptons leaving the outer-magnetosphere accelerator that then flows toward the stellar polar cap. This perpendicular energy ($cp_\perp \equiv \gamma_\perp mc^2$) will be lost to synchrotron radiation in the increasing magnetic field nearer the star and leave a reduced $\gamma(R) \sim \gamma_a/\gamma_\perp$ when the star is reached. This is not expected for the Crab pulsar because the outer-magnetosphere field strength $B \sim 10^6$ G, sufficiently large that synchrotron radiation will remove $\gamma_\perp$ even before acceleration to γ_a is accomplished. However, the outer magnetosphere in the more slowly rotating Geminga pulsar may have a much weaker field (typically, with half the dipole field and 9 times the period of the Crab pulsar, the magnetic field in Geminga's outer magnetosphere may be smaller by a factor $9^{-3}/2 \sim 7 \times 10^{-4}$). If primary pairs in the outer magnetosphere are produced by collisions of GeV (curvature) γ-rays on soft X-rays (probably from the stellar surface), the initial $\gamma_\perp \equiv p_\perp/mc \sim 10^2$–$10^3$. However, even if it is not immediately quenched by synchrotron radiation, acceleration along the curved outer-magnetosphere $\boldsymbol{B}$ will greatly suppress it. The drag force on a spiraling electron in the accelerator is directed almost exactly opposite in direction to the instantaneous momentum vector of the electron, while the average accelerating electric field is effective only in the direction parallel to the local $\boldsymbol{B}$. It follows that $\gamma_\perp$ will be diminished during acceleration along the curved $\boldsymbol{B}$-field line;

$$\gamma_\perp(s) = \gamma_\perp(0) \exp\left(-\frac{s}{\rho_c}\frac{2e^2\gamma^3}{3mc^2\rho_c}\right), \quad (42)$$

where ρ_c^{-1}, the total trajectory curvature, includes both that from $\gamma_\perp$ and that from the constrained (averaged) motion along the curved $\boldsymbol{B}$; s is the distance the electron has moved after its creation with an initial perpendicular momentum component $p_\perp = \gamma_\perp mc$. For typical values $s/\rho_c \simeq \frac{1}{2}$ and $\gamma^2 \simeq 10^{15}$, $\gamma_\perp(s) \simeq \gamma_\perp(0)e^{-3}$. Thus, for Geminga with an initial $\gamma_\perp(0) \sim 5 \times 10^2$, $\gamma_\perp(r_a) \sim 25$. Then, although the total electron γ when leaving the accelerator is $\sim 3 \times 10^7$, it is soon reduced by synchrotron radiation quenching of $\gamma_\perp$ to about 10^6. (There is some additional reduction of total γ as some γ is transferred into $\gamma_\perp$ by the converging field lines.) If indeed $\gamma(R) = 10^6$, $L_x \sim 5 \times 10^{31}$ ergs s^{-1}. The discrepancy with the observed L_x would no longer be a serious problem. On the other hand, the greatly reduced γ would suppress curvature γ-ray radiation energetic enough to give the two generations of $e^{\pm}$ pairs created in the Crab magnetosphere.

2. The particle flow from the accelerator down toward the polar cap may be very much less than the Goldreich-Julian limit, e.g., $\dot{N}_a \leq 10^{-1}\dot{N}_{GL}$. However, it is difficult to construct an outer-magnetosphere accelerator that spans a small fraction f of the accessible open field lines that would not then also reduce the accelerator potential (ΔV) by a similar factor f, or even more likely by f^2. Then the total outer-magnetosphere accelerator γ-ray emission power $P_\gamma \sim (f^2 \text{or } f^3)I\Omega\dot{\Omega}$. This would not be compatible with Geminga observation unless there is very strong beaming in the γ-ray emission (e.g., Dermer & Sturner 1991).

3. Magnetic field line curvature near the star may greatly exceed that from a pure central dipole. If, for example, the curvature radius near the star were to be r instead of $(rc/\Omega)^{1/2}$, the energy per primary particle striking the polar cap would be reduced from 6.5 ergs to about 1 erg (assuming the curvature γ-rays emitted above the star largely miss its surface.)

Because of the first of the above three considerations, the best candidates for strong γ-ray annihilation lines similar to that claimed for the Crab pulsar may be those γ-ray pulsars that have similar outer-magnetosphere $\boldsymbol{B}$. Then the inward flowing primaries that have passed through the accelerator should not have an important $\gamma_\perp$ (which, after subsequent synchrotron radiation, will reduce the primary energy by a factor $\sim\gamma_\perp^{-1}$). For a large tilt angle ϕ between $\boldsymbol{\Omega}$ and the neutron star dipole moment, the largest "null-surface" local $\boldsymbol{B}$ is given by (Ruderman et al. 1993)

$$B \sim B_p\left(\frac{R\Omega}{c}\right)^3\left(\frac{9}{4}\right)^3 \tan^6\phi . \quad (43)$$

The sensitivity of B to ϕ when ϕ is large makes it difficult to predict this B with confidence, even for slower γ-ray pulsars like Geminga. However, the most likely candidates for large B may be γ-ray pulsars with the large Ω (e.g., the Crab with $\Omega \simeq 190\text{s}^{-1}$ and $B_p \simeq 3 \times 10^{12}$ G) or large B_p (e.g., PSR 1509−58 with $\Omega \simeq 40\,\text{s}^{-1}$ and $B_p \simeq 2 \times 10^{13}$ G). If this B is sufficiently large, the number of annihilating pairs should scale roughly as the flow rate of primaries from the accelerator to the star ($f\Omega^2BR^3/ec$).

We are happy to thank J. Halpern, K. S. Cheng, E. Massaro, and B. Agrenier for helpful conversations, M. Ulmer for discussions about OSSE observations, and C. Dermer for very valuable comments, criticism, and guidance. This work is supported in part by NASA grants NAG 5-2016 and NAG 2841.

REFERENCES

Agrenier, B., et al. 1990, ApJ, 355, 645
Arons, J. 1981, in IAU Symp. 95, Pulsars, ed. W. Sieber & R. Wielebinski (Dordrecht: Reidel), 69
Ayre, C. A., Bhat, P. N., Ma, Y. Q., Myers, R. M., & Thompson M. G. 1983, MNRAS, 205, 285
Bednarek, W., Cremonesi, O., & Treves, A. 1992, ApJ, 390, 489
Bignami, G. F., Caraveo, P. A., & Mereghetti, S. 1993, Nature, 361, 704
Blandford, R. D., & Scharlemann, E. T. 1976, MNRAS, 174, 59
Cheng, A., & Ruderman, M. A. 1977, ApJ, 216, 865
Cheng, A., Ruderman, M. A., & Sutherland, P. G. 1976, ApJ, 203, 209
Cheng, K. S., Ho, C., & Ruderman, M. 1986a, ApJ, 300, 500
———. 1986b, ApJ, 300, 522
Clear, J., Bennett, K., Buccheri, R., Grenier, I. A., Hermsen, W., Mayer-Hasselwander, H. A., & Sacco, B. 1987, A&A, 174, 85
Dermer, C. D., & Sturner, S. J. 1991, ApJ, 382, L23
Goldreich, P., & Julian, W. H. 1969, ApJ, 157, 869
Haplern, J. P., & Ruderman, M. 1993, ApJ, 415, 286
Harris, M. J., Share, G. H., & Leising, M. D. 1994, ApJ, 420, 649
Leventhal, M., MacCallum, C. J., & Watts, A. 1977, ApJ, 216, 491
Massaro, E., et al. 1991, ApJ, 376, L11

Owens, A. 1990, in AIP Conf. Ser. 232, Gamma-Ray Line Astronomy, ed. N. Prantzon & P. Durchoux (New York: AIP), 341
Owens, A., Myers, R. M., & Thompson, M. G. 1985, 19th Int. Cosmic Ray Conf. (Greenbelt), 1, 145
Ruderman, M. A., Chen, K., Cheng, K. S., & Halpern, J. P. 1993, in AIP Conf. Ser. 280, *Compton Gamma Ray Observatory*, ed. N. Gehrels & M. Friedlander (New York: AIP), 259
Ruderman, M. A., & Sutherland, P. G. 1975, ApJ, 196, 51
Sturner, S. J., & Dermer, C. D. 1994a, A&A, 284, 161
———. 1994b, ApJ, 420, L79
Sturrock, P. 1971, ApJ, 164, 529
Ulmer, M. P. 1996, private communication
Wills R. D., et al. 1982, Nature, 296, 723
Yoshimori, M., Mahoney, W. A., Willett, J. B., & Murakami, H. 1979, Australian J. Phys., 32, 375